My First Autonomous Car

Driver: Yuto Watanabe
Crew Chief: David Llanos
Owner: Kaley Boyce
Pit Boss: Ben Jensen

Part 1.1: Speed Profile Design

The speed profile along the path was optimized to achieve the fastest time of completion. The goal was to create the speed profile as a function of the location (s), given the curvature (κ) along the path. There were four constraints that limited the speed along the path:

1. Maximum speed is limited to 10 m/s
2. The vehicle must stop at the end of the path
3. Lateral acceleration must be less than 0.3 g
4. Longitudinal acceleration must be less than 0.2 g

In order to satisfy these four constraints, we first separated the constraints that are only a function of s, which includes the first three constraints.

The first is trivial since it is a constant,

$$v_{max} = 10 \text{ m/s}$$

The second is also trivial since it is a boundary condition,

$$v_{max@\ end} = 0\ m/s$$

The third constraint involves some consideration of dynamics. Assuming that the car has small sideslip (i.e. the car is facing tangent to the path), the lateral acceleration can be written as

$$a_{lat} = \frac{v^2}{r} = \kappa v^2$$

where r is the local radius of the path and κ is the local curvature of the path. Since in this case the lateral acceleration is our limiting factor, we can rearrange the equation to

$$v_{max,a_{lat}} = \sqrt{\frac{a_{lat}}{|\kappa|}}$$

Since v_{max,v_x}, $v_{max@\ end}$, and $v_{max,a_{lat}}$ are all functions of only s, a velocity profile can be made with each of these three constraints.

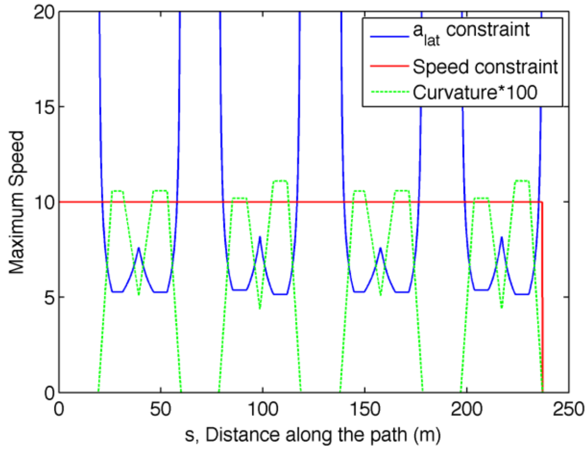

The plot shows each of the components of the velocity constraints for the Searseville Oval path. The speed constraint due to curvature increases as curvature increases, and is infinite when the path is straight, because in that case there is no lateral acceleration. The dip in the speed constraint at end is due to the constraint that the velocity must be 0 m/s at the end. All of the constraints can be met by taking the minimum of the components for every location. This process creates the following velocity profile.

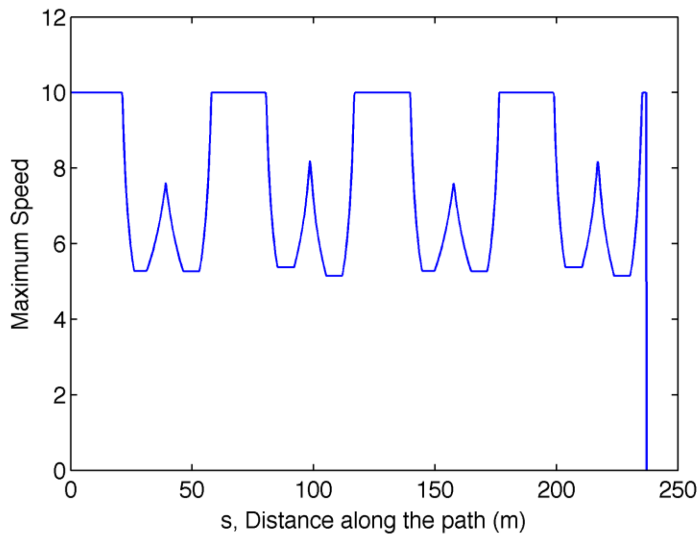

This velocity profile, however, does not include the constraint of longitudinal velocity. This constrained is more complicated than the earlier constraints since it is not only a function of location.

In order to generate a speed profile that is within the longitudinal acceleration constraint, an algorithm was developed. The algorithm starts at the beginning of the path and simulates the velocity and acceleration of the vehicle as it traverses to the end of the path. For each step of the simulation, the vehicle advances one step in distance. At the start of the path, the velocity is 0 m/s. As the simulation advances through the path, it simulates its projected speed trajectory if the vehicle were to decelerate at its maximum rate (0.2 g). Depending on if the projected speed trajectory goes faster than the speed profile given above, it chooses between 3 options

a) If the projected speed profile is faster than the speed profile, the vehicle decelerates as it moves to the next distance step.
b) If the projected speed profile is slower than the speed profile, it has two options
   i. If it is already at the maximum speed, it will follow the maximum speed for the next step.
   ii. If it is not at the maximum speed, it will accelerate at its maximum acceleration.

This algorithm produced some discontinuities in the lateral acceleration when the curvature profile for the path was not smooth. Therefore some filtering was done to remove the discontinuities.

The algorithm produced the following desired speed profile and lateral acceleration profile:

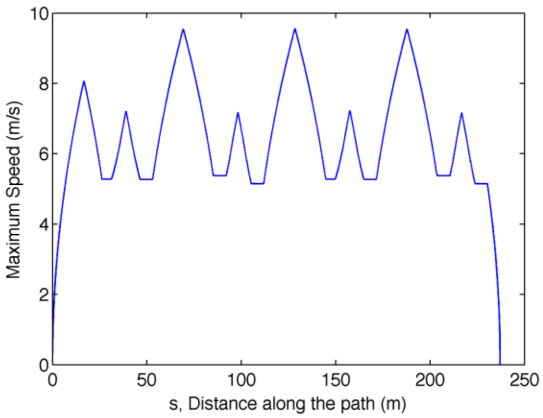

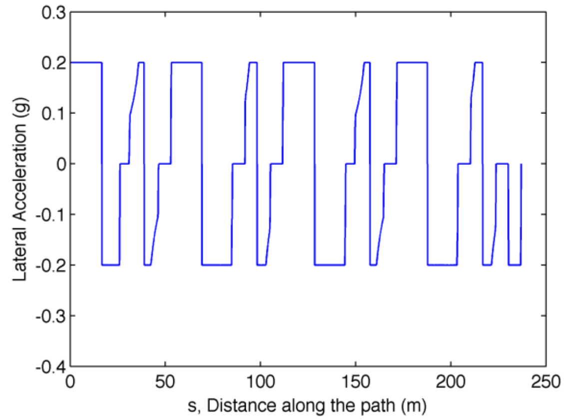

This speed profile meets all of the constraints for the velocity. The lateral acceleration is at the maximum limit for a large portion of the time, indicating that it is speeding up or slowing down as fast as it can to travel the path the fastest it can.

Part 1.2: Steering and Speed Controller Design

The steer-angle and speed controller was designed largely based on what was discussed in class.

Steer-Angle Controller

The steer angle controller was comprised of a feedback controller based on the lookahead distance, and a feedforward controller based on the linear handling diagram. The feedback control law was designed the following:

$$\delta_{FB} = -k_p(e + x_{LA}(\Delta\Psi + \beta_{SS}) + \frac{\kappa}{2}k_s^2)$$

The lookahead controller takes into account the side-slip error for steady state condition using the understeer gradient using the β_{SS} term.

$$\beta_{SS} = -\frac{mU_x^2 a}{C_r L}\kappa + b\kappa$$

The original lookahead controller covered in class calculates a lookahead error assuming that the road continues straight in the direction tangent to the path. However with tight turns and long lookahead distances, this could be a poor assumption. By using the local curvature of the road as a second order derivative, the controller could better approximate the lookahead error by assuming that the road is a parabolic shape, rather than a line. The second order term is included in the control law as $\frac{\kappa}{2}k_s^2$,where k_s is the second order gain. In theory k_s should be the same distance as x_{LA} according to Taylor series approximation, though in simulation we found that this overcompensated the lateral error. Therefore, we decided to make it a smaller distance and represent it as another tunable parameter. In addition, this let us make k_s a negative value in the case the car was turning too much into the corner.

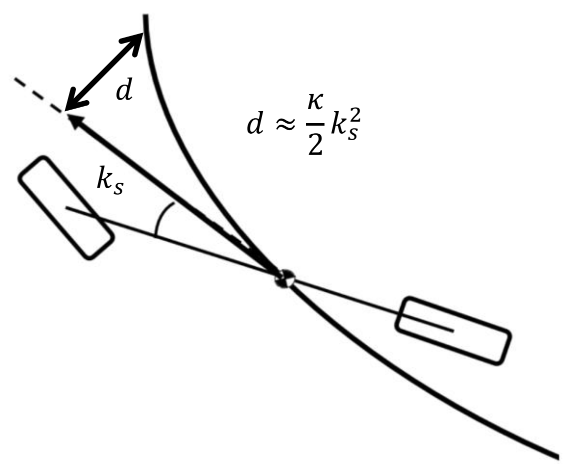

A feedforward controller was also implemented, since the lateral force acting on the vehicle could easily be approximated using the lateral velocity and curvature of the path. The feedforward term was implemented as

$$\delta_{FFW} = L\kappa + K_{ug}\frac{U_x^2\kappa}{g}$$

The output of the steer angle controller was the sum of the feedback and feedforward terms

$$\delta = \delta_{FB} + \delta_{FFW}$$

Speed Controller

The speed controller controlled the lateral tire forces, was also comprised of a feedback controller and a feedforward controller.

The feedback controller was designed as a proportional controller based on the current vehicle speed and the desired vehicle speed according to the speed profile discussed earlier. This controller was implemented as

$$F_{x,FB} = k_x(U_x - U_{x,des})$$

The feedforward controller for the vehicle was also relatively straightforward. The velocity profile generation algorithm also outputted a desired acceleration along the path. This desired acceleration was used to in the feedforward controller to achieve a vehicle speed that did not lag behind the desired speed.

$$F_{x,FFW} = mA_{x,des}$$

Again, the speed controller outputted the sum of the feedforward and feedback terms.

$$F_x = F_{x,FB} + F_{x,FFW}$$

Controller Tuning

In the speed and steer-angle controller, there are four tunable parameters: k_p, x_{LA}, k_s and k_x. Even without using the second order lookahead term, the controller worked pretty well with the parameters specified in homework 4. Therefore, we did not change those values. However, we did tune k_s, which is the gain that is associated with the second order lookahead term. Several iterations were done in simulation to choose a value for k_s that minimizes the maximum lateral error.

The following are the gains we used for our first test run:

$$k_s = 0.1 \text{ m}$$
$$x_{LA} = 12 \text{ m},$$
$$k_x = 2000 \text{ N},$$
$$k_y = 14000 \text{ N}$$

Part 2.1: Simulation and Experimental Results

Using our designated controller method and speed profile, explained in the previous section, we ran simulations to measure the following parameters as a function of the position: the simulated and desired speed, the longitudinal speed error, the desired and simulated longitudinal acceleration and the desired and simulated lateral acceleration. Also included, as a function of time, were the lateral and heading error. The following figures display the simulated and experimental values.

Simulated Data

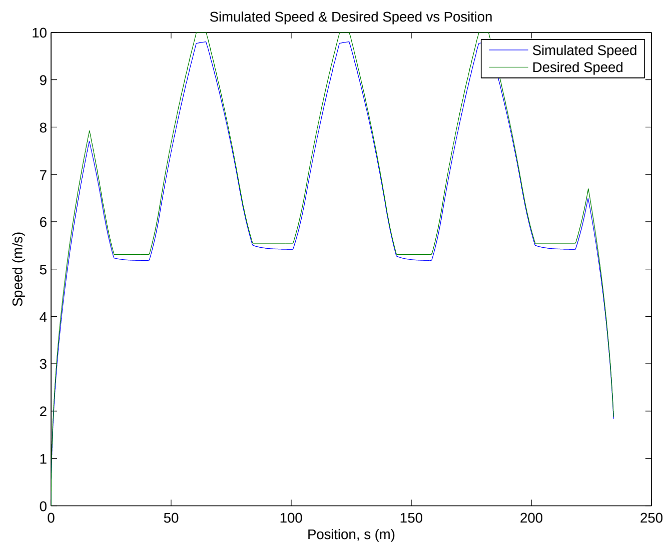

Figure 2.1. Simulated speed and desired speed vs. position.

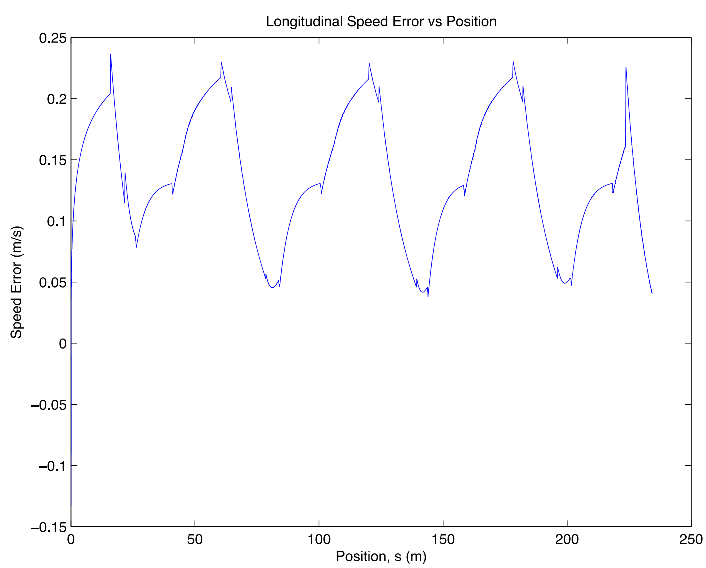

Figure 2.2. Simulated longitudinal speed error vs. position.

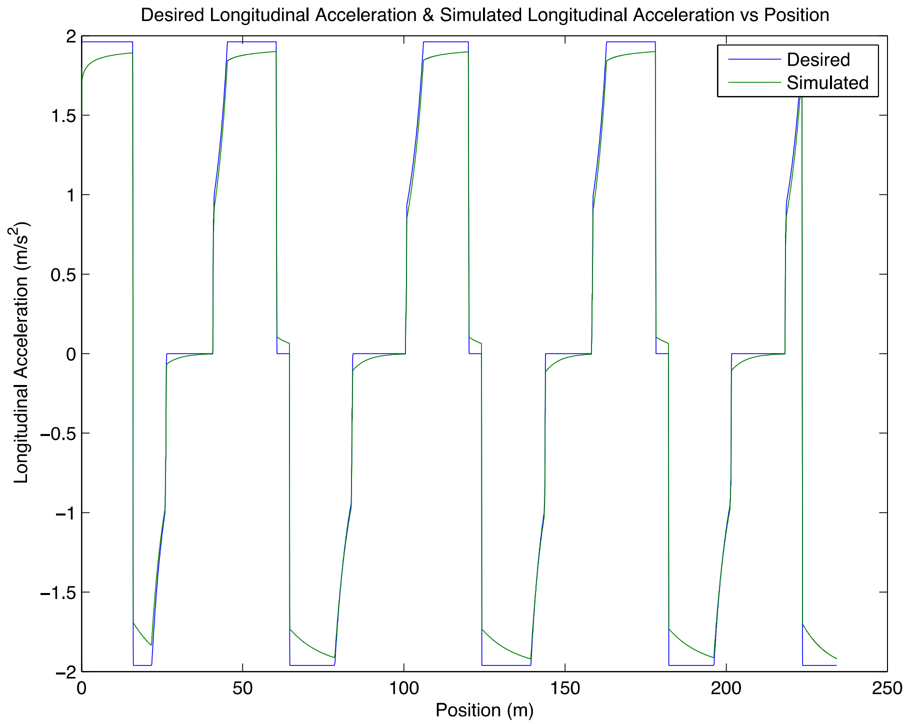

Figure 2.3. Simulated longitudinal acceleration and desired longitudinal acceleration vs. position.

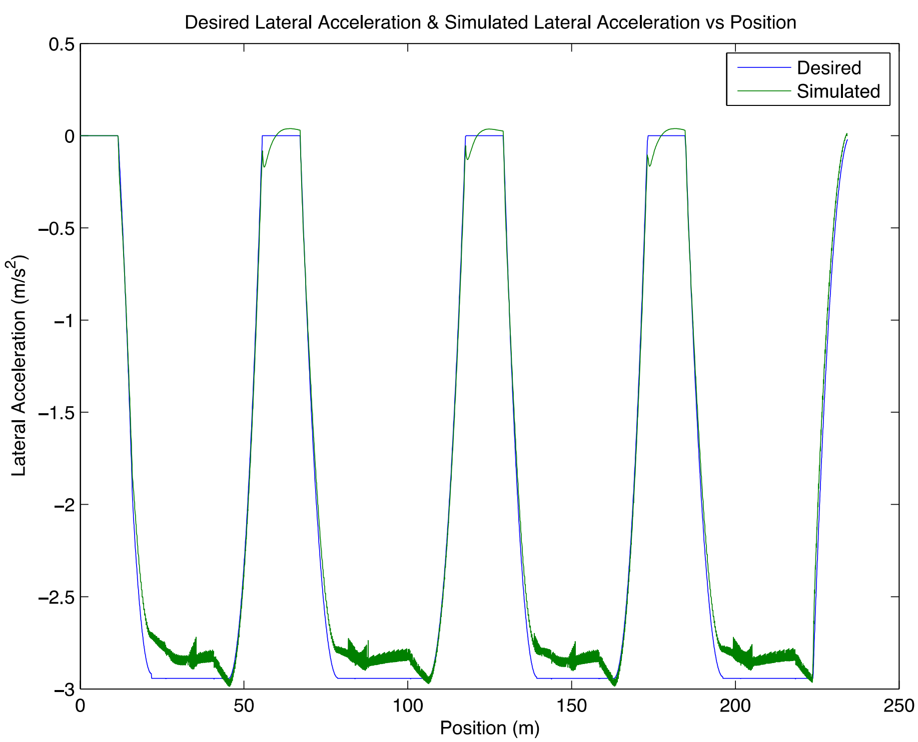

Figure 2.4. Simulated lateral acceleration and desired lateral acceleration vs. position.

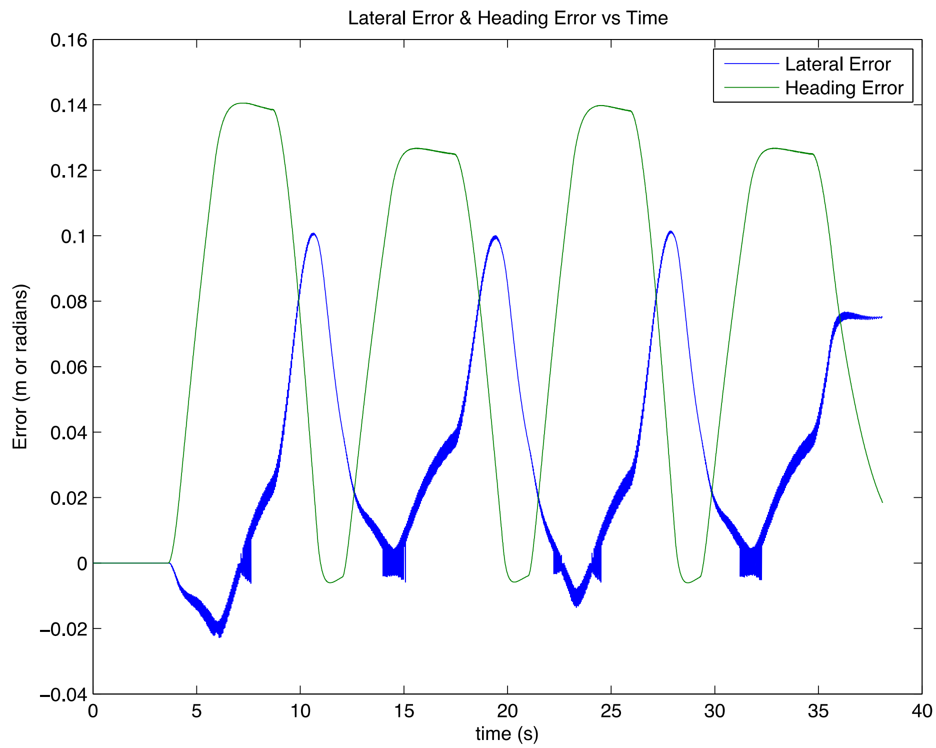

Figure 2.5. Simulated lateral error and heading error vs. time.

Exhibited in Fig. 2.1, the simulated and desired speed tracking results holds very well. Our profile and controller design successfully helped to minimize speed error. In Fig. 2.2 when measuring the speed error we see a maximum speed error of 0.25 m/s. The simulated and desired longitudinal and lateral accelerations, displayed in Fig. 2.3 and 2.4, respectively, also match up very well. The simulation follows the desired profile very well with low deviations and error. In Fig. 2.5 we can see that for the lateral error the maximum value is approximately -0.02 m. The heading error maximum value is approximately 0.14 radians.

Experimental Data

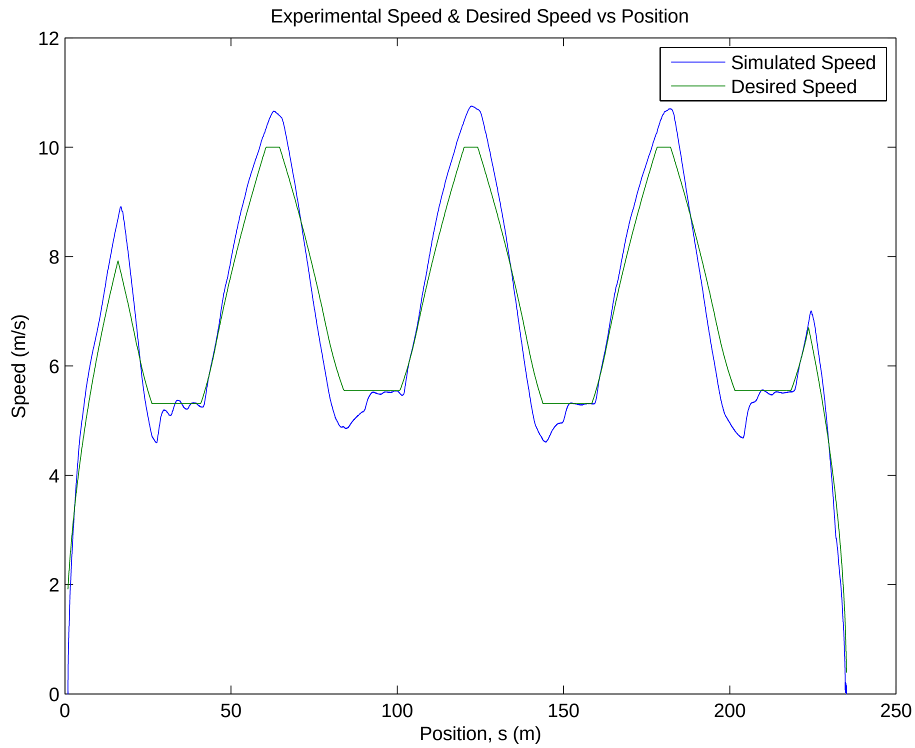

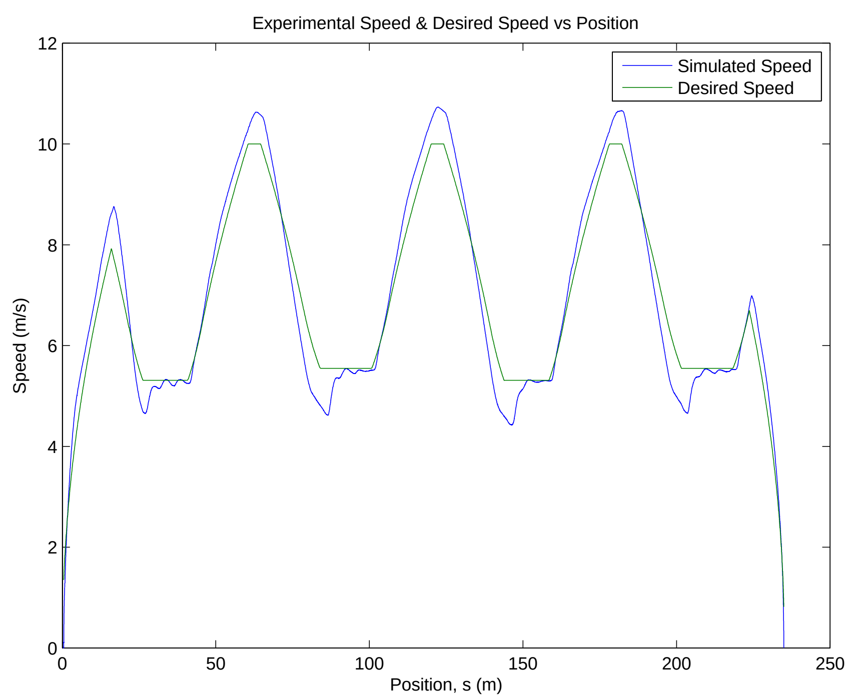

Figures 6a & 6b. Experimental speed and desired speed vs. position for run 1 and run 2.

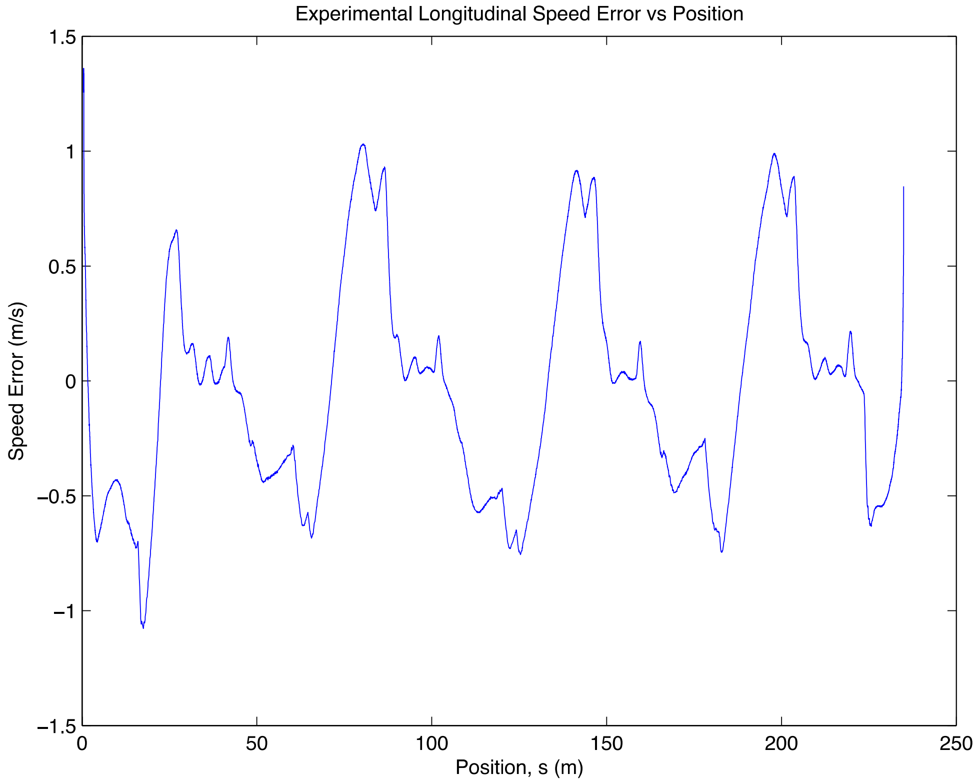

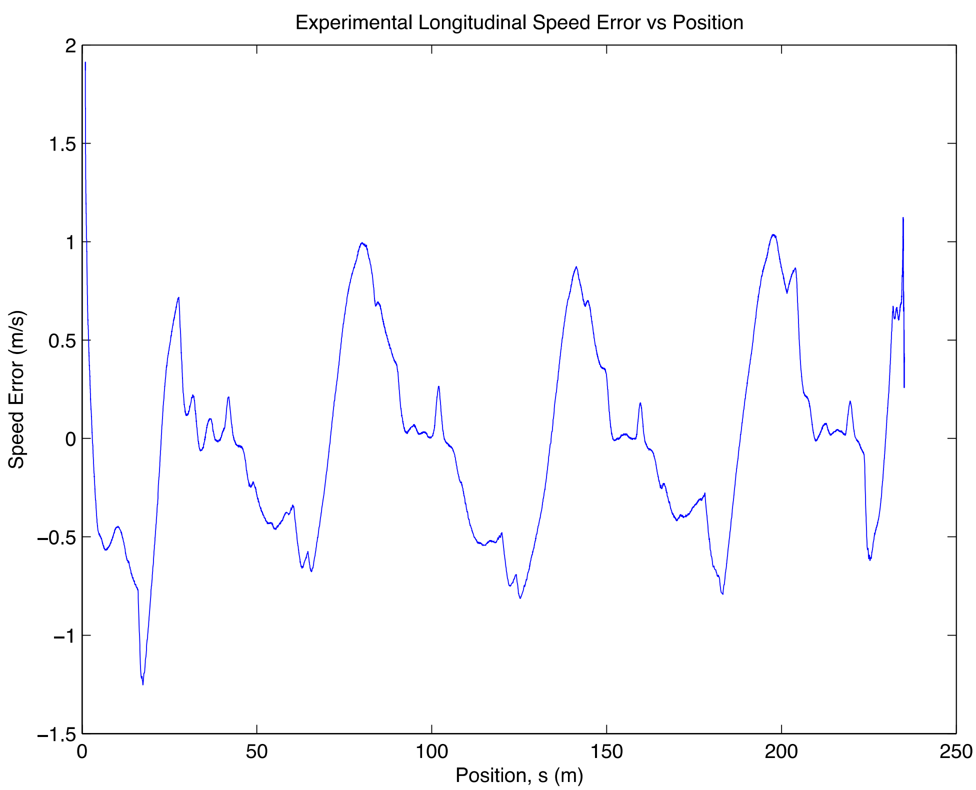

Figures 7a & 7b. Experimental longitudinal speed error vs. position for run 1 and run 2.

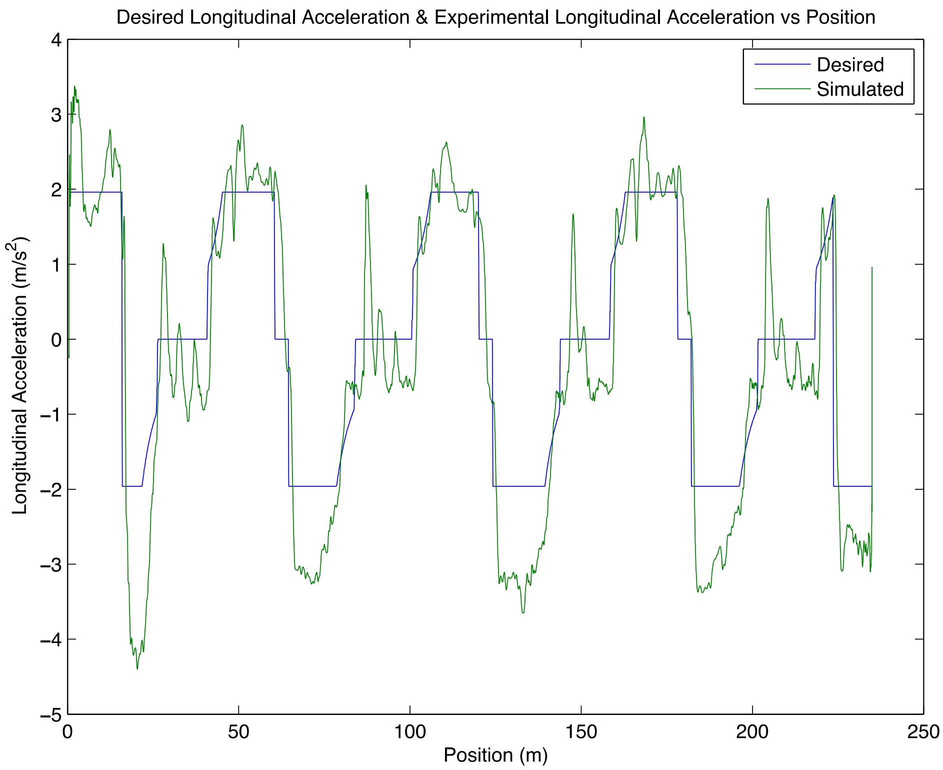

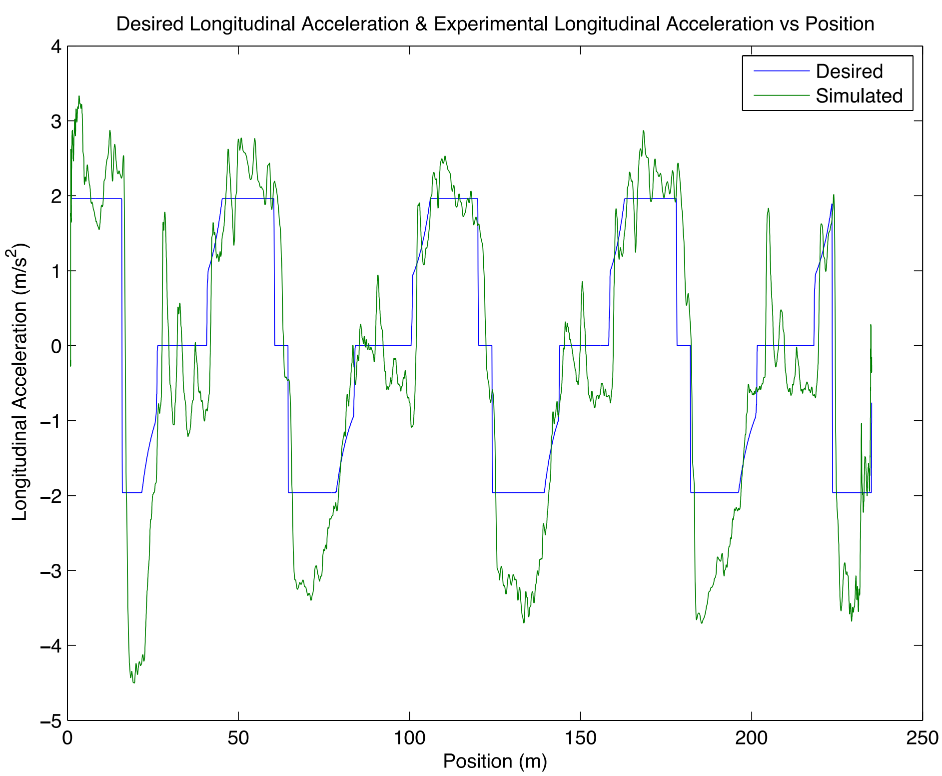

Figures 8a & 8b. Experimental longitudinal acceleration vs. position for run 1 and run 2.

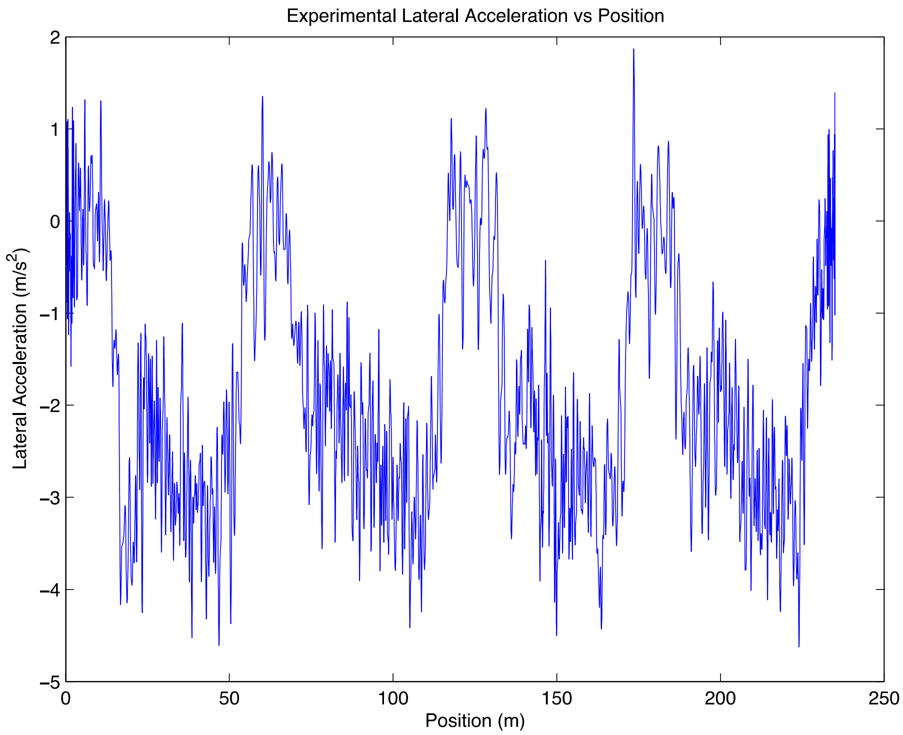

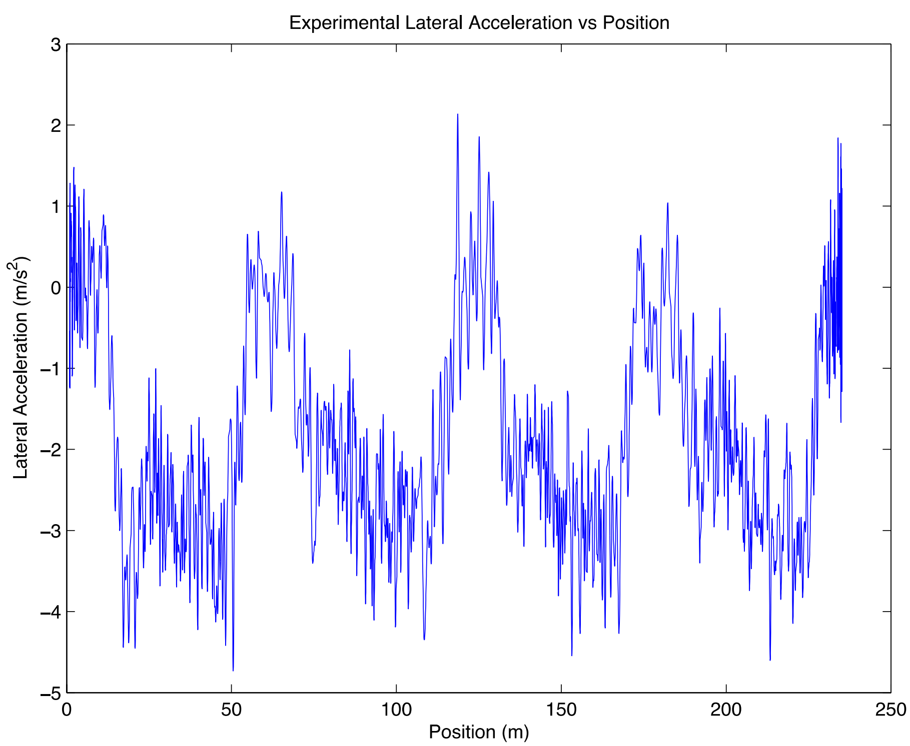

Figures 9a & 9b. Experimental lateral acceleration vs. position for run 1 and run 2.

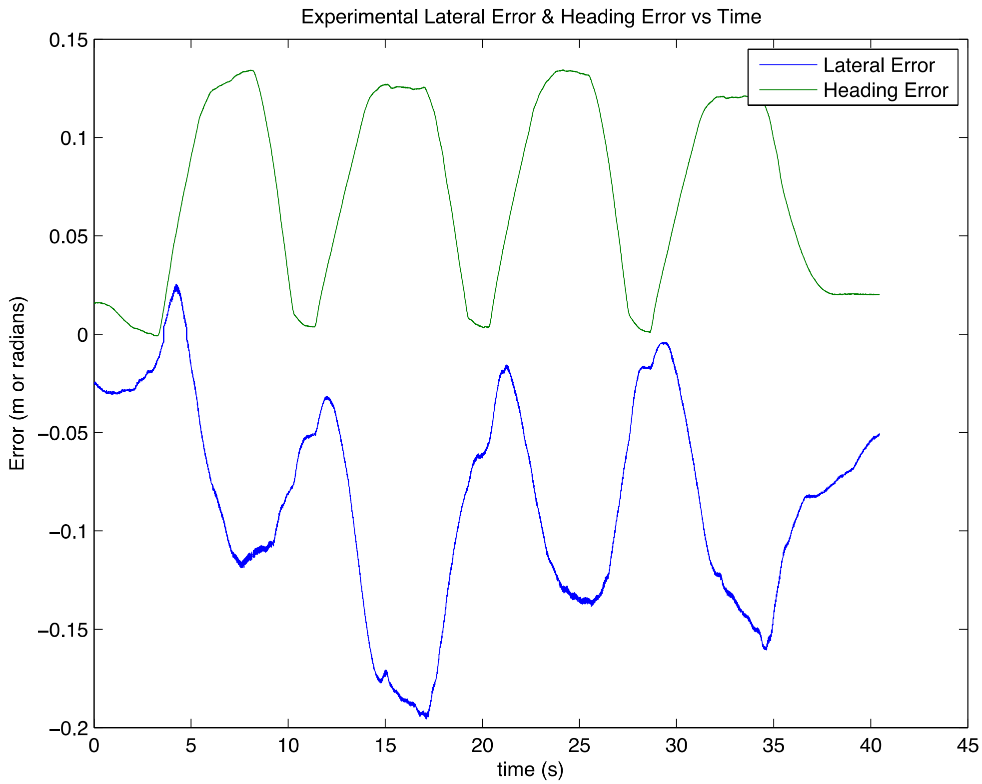

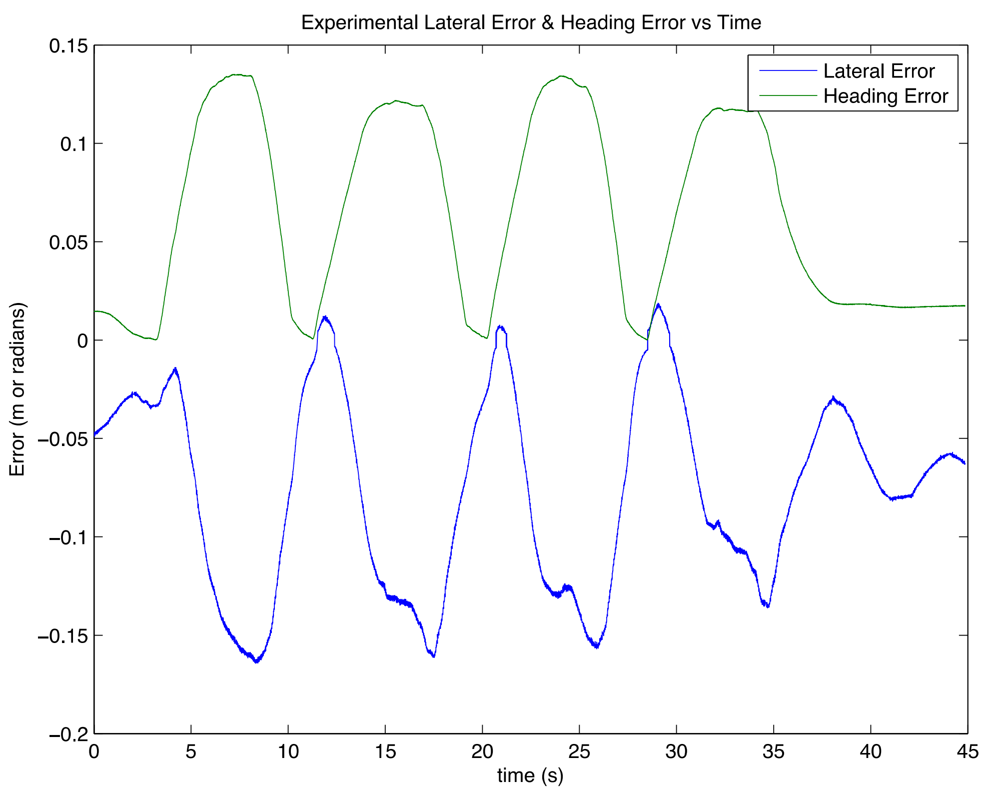

Figures 10a & 10b. Experimental lateral & heading error vs. time for run 1 and run 2.

As can be seen from figures 6 - 10, the speed profile and controller, still do an adequate job of predicting velocities, accelerations, and the path profile, but although comparable to simulated values the experimental data introduce more error and variation in results.

In figs. 6a and 6b (no visible difference between the two runs) the experimental speed follows the desired speed in general shape but there is a visible difference particularly after every deceleration, which corresponds to the turns. Looking at Fig. 7a and 7b we can trace the error in speed tracking to the deceleration portions of the path where we see a maximum speed error of about 1 m/s. Comparing the two figures we can see a slight improvement in run 2 after implementing the changes to the controller, as the split peaks visible in fig. 7a at the turns are less pronounced in fig. 7b.

Turning to Fig. 8a and 8b, again we can see the same general trends seen before. Our general longitudinal acceleration tracking was acceptable, but did not match the desired longitudinal acceleration within up to 2 m/s^2. Again the same improvement is seen from run 1 to run 2 as many of the split peaks observed in the first figure are dulled or removed in figure 2. In Fig. 9a and 9b, we observe sharp differences in lateral accelerations throughout the entire track. A possible explanation for this “noise” is that in actuality these readings are accurate but measure much of the vibrational frequencies depending on where the accelerometer was positioned. No visible improvements were seen from run 1 to run 2.

Finally, in Fig. 10a and 10b, we see that the heading error has remained close to our simulated values from fig. 5, but our maximum lateral error has increased by about a factor of four. After the changes were made to the controller, from run 1 to run 2 we observe approximately a 25 percent decrease in lateral error. One possible reason for the continued error is that our simulation did not take into account any changes in grade for the track. From observing the track during testing, it is clearly visible that the Searsville track experiences slight changes in grade throughout some of the straightaways and turns which might indicate at least a possible reason for the differences between the simulated and experimental results. Overall our experimental data compares favorably with simulation and although we expected slight differences, there are a variety of possible reasons as to why they occurred such as grade not being accounted for and placement of measuring equipment on the vehicle.

PART 3: Results from Updating Code during Experiment

Because our first test performed very well with respect to speed tracking, our group chose to try to tackle the relatively large lateral error we were experiencing during the turns. From our simulation, we were expecting to see a maximum lateral error of 10cm (see Fig. 5), but during our test we found that the car was tracking the path on the inside more than we expected. As observed in Fig. 10a, the car generally stayed on the inside of the turns, and we experienced a maximum lateral error of approximately -19cm, almost double what we expected.

Since this lateral error was most apparent during the turns, our group decided to edit the gain of the curvature lookahead term we added to our steer angle control law, as discussed in Part 1. We postulated that our controller was overcompensating for the turn by increasing the steer angle too much for the given curvature.

In our controller, we included the term: $\frac{K_{Kla}{}^2}{2} * abs(\kappa)$ where K_{Kla} is the gain, and κ is the road curvature. For our first test, the sign of this term was positive, and the magnitude of our K_{Kla} term was 0.1. To mitigate the largely negative lateral error for the next test, we changed the sign and magnitude of this term, such that the lateral error would become more positive and our car would move towards the outside of each turn *(* $- \frac{K_{Kla}{}^2}{2} * abs(\kappa)$*,* $K_{Kla} = 0.5$*).*

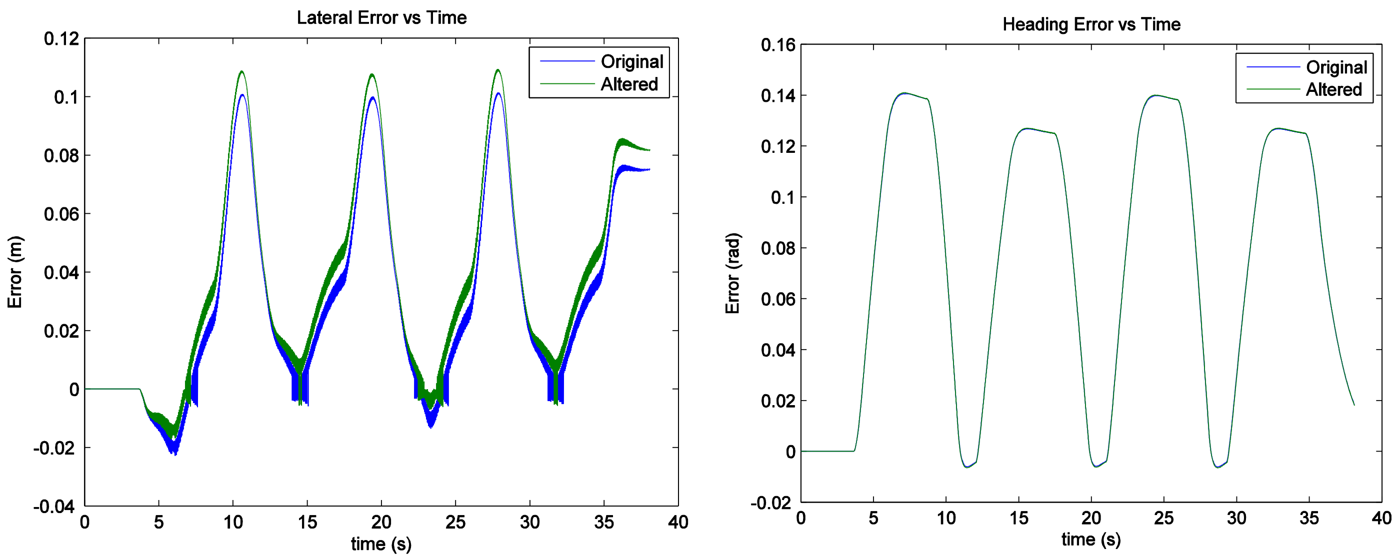

Figure 11a & 11b. Simulation of Lateral and Heading Error for Original and Altered Controller

As seen in Fig. 11a, making this alteration to our steer angle control law pushed the magnitude of the lateral error higher, to approx. 11cm. We did this in order to compensate for the extremely negative values of lateral error experienced during our test run, in an effort to push the lateral error more positive. By increasing the lateral error in simulation, we hoped to mitigate the negative values of lateral error in simulation. This change in steer angle control law had no effect on the expected heading error in simulation (see Fig. 11b).

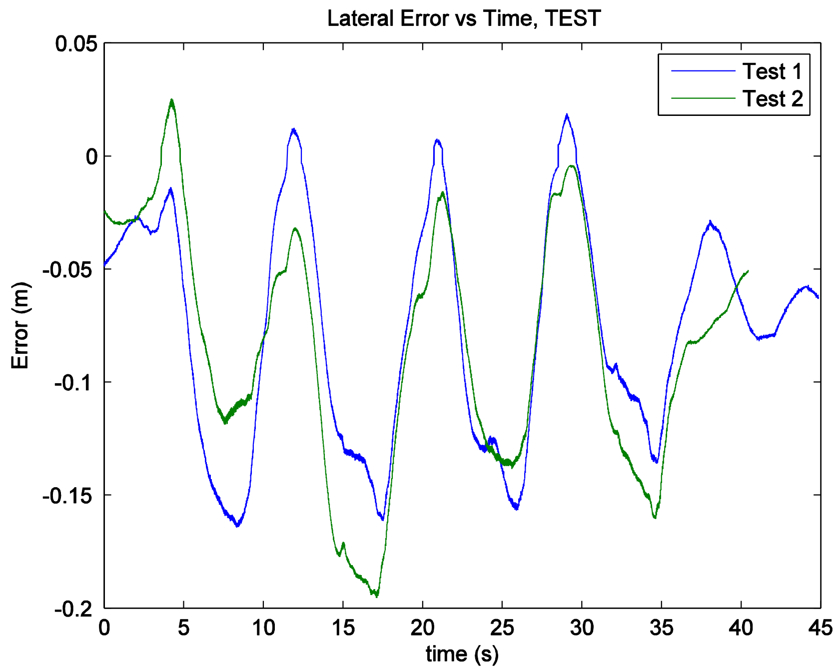

Figure 12. Test results before and after alteration of controller

As observed in Fig. 12, the alteration to the controller improved the Lateral Error behavior on the first turn on the track, but worsened it on the second turn.

PART 4: What We Learned!

In the course of this project we were able to develop control laws for heading and longitudinal speed, use a bicycle model type vehicle simulation and experimentally test and validate them on Shelley. For the speed profile, we develop an algorithm to predict speed based on a projected speed profile and accelerated or decelerated in order generate the fastest lap time around the given constraints. In our control law design, we develop additional terms which helped us better adjust our feedback term for our steering control and used a feedback - feedforward controller for our longitudinal speed controller. Through simulation we tuned and adjusted our gains based on the course map and prepared for experimental testing. Through experimental testing we discovered that our control laws worked quite well (as predicted in our simulation) and gave us an initial maximum lateral error of -19 cm and heading error of 0.14. This turned out to be a bit more than we predicted in simulation. We adjusted our control laws in order to try to mitigate the negative values of lateral error in simulation we found experimentally, but found that the change in steering control had no effect on heading error in simulation.

Finally, we had a lot of fun having the opportunity to play with Shelley and we appreciate you allowing us to do this for our midterm project!

Final Results: